

# A NEW GENERAL ACTIVE SNUBBER CELL FOR DC/DC CONVERTERS

S.H. Hosseini  
email: [hosseini@tabrizu.ac.ir](mailto:hosseini@tabrizu.ac.ir)

R. Moradi

H. Javidnia  
email: [hooman.javidnia@ieee.org](mailto:hooman.javidnia@ieee.org)

*Electrical Engineering Department, Faculty of Engineering, University of Tabriz, 51664, Tabriz-Iran*

## ABSTRACT

A new soft switching active snubber cell with constant configuration is proposed. The proposed active snubber uses an auxiliary switch to recover stored energy in the snubber capacitor during turn off of the main switch. Complete analysis for the boost converter is given and the results obtained for other DC/DC converters are reported. Soft switching commutation is achieved for all semiconductor devices and consequently the switching losses and electromagnetic interference (EMI) are considerably reduced. Both simulation and experimental results are presented.

## I. INTRODUCTION

Pulse Width Modulated (PWM) converters have been widely used in industry. The PWM technique is praised for its high power capability and ease of control. Higher power density, faster transient response and smaller physical size of PWM converters can be achieved by increasing the switching frequency. However, as the switching frequency increases so do the switching losses and electromagnetic interference (EMI) noises. Switching losses and EMI noises of PWM converters are mainly generated during turn-on and turn-off transients [1]. Resonant converters commute with either zero-voltage-switching (ZVS) or zero-current-switching (ZCS) to reduce switching losses and EMI noises.

A few zero-voltage-transition (ZVT)-PWM and zero-current transition (ZCT)-PWM techniques were proposed to combine desirable features of both the conventional PWM converters and resonant converters [2-6]. They are generally implemented by adding active snubbers, which employ resonant techniques to PWM converters. Switching losses and EMI noises are reduced because the converters operate at either ZVS or ZCS.

This paper introduces a new generic active snubber cell for DC/DC converters. Soft switching is achieved for semiconductor devices not only in the original converters, but also in the snubber cell. As an example, a study of a boost converter equipped with the proposed snubber cell is investigated in depth. Steady state operation analysis and relevant equations are presented in detail. Finally the proposed implementations of active snubber have been simulated and experimentally tested.

## II. THE BOOST CONVERTER WITH AN ACTIVE SNUBBER

Figure 1 shows the proposed snubber topology for the boost converter. The proposed configuration achieves zero-voltage switching for the main switch and zero-current switching with zero-voltage at turn-off for the auxiliary switch. Furthermore, there is no reverse-recovery problem for the main diode since its current decreases linearly.

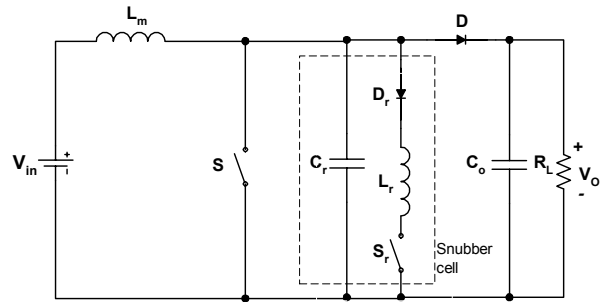


Fig.1. The boost converter with active snubber

The equivalent circuits of six modes of operation are shown in Figure 2 and the basic predicted waveforms are shown in Figure 3.

To analyse the steady state operation of the proposed mixed converter, the following assumptions are made:

- 1) The output capacitor  $C_o$  is large enough to assume that the output voltage  $V_o$  is constant and ripple free.
- 2) The main inductor  $L_m$  is large enough to be treated as a constant-current source  $I_{L_m}$ .
- 3) Main inductor  $L_m$  is much greater than resonant inductor  $L_r$ .
- 4) The semiconductor devices and the reactive elements are ideal.

The operation of the circuit over one switching cycle is described in the following six modes:

### MODE 1

$$t_0 < t < t_1 \text{ (Figure 2a)}$$

During this mode of operation, switch  $S$  is in conduction and supplying energy to the main inductor  $L_m$ . Using the

equivalent circuit of Figure 2a, the following equations are obtained:

$$v_{cr}(t) = 0 \quad (1)$$

$$i_{Lr}(t) = 0 \quad (2)$$

$$v_{Lm}(t) = V_{in} \quad (3)$$

This mode ends at  $t = t_1$  as switch  $S$  turns off.

### MODE 2

$$t_1 < t < t_2 \quad (\text{Figure 2b})$$

When switch  $S$  turns off, capacitor  $C_r$  is charged linearly and zero-voltage turn-off is achieved for the main switch. Furthermore the voltage across diode  $D$  is decreasing linearly from  $-V_0$  to zero at the end of this mode. Therefore, zero-voltage turn-on for the diode  $D$  will be achieved. Moreover, during this mode of operation switch  $S_r$  and diodes  $D_r$  and  $D$  are still not conducting. Using the equivalent circuit of Figure 2b the following equations are obtained:

$$v_{cr}(t) = \frac{I_{Lm}}{C_r}(t - t_1) \quad (4)$$

$$i_{Lr}(t) = 0 \quad (5)$$

$$v_{Lm}(t) = V_{in} - \frac{I_{Lm}}{C_r}(t - t_1) \quad (6)$$

This mode ends when  $v_{cr}(t_2) = V_0$  and consequently the time interval of this mode is given by:

$$t_{21} = t_2 - t_1 = \frac{V_0}{I_{Lm}} C_r \quad (7)$$

### MODE 3

$$t_2 < t < t_3 \quad (\text{Figure 2c})$$

During this mode the current of the main inductor flows through diode  $D$  and the load. Mode 3 ends when switch  $S_r$  turns on at the instant  $t = t_3$ . Using the equivalent circuit of Figure 2c, the following equations are obtained:

$$v_{cr}(t) = V_0 \quad (8)$$

$$i_{Lr}(t) = 0 \quad (9)$$

$$v_{Lm}(t) = V_{in} - V_0 \quad (10)$$

### MODE 4

$$t_3 < t < t_4 \quad (\text{Figure 2d})$$

This mode starts when switch  $S_r$  turns on at  $t = t_3$ . The resonant inductor current  $i_{Lr}$  is increasing linearly from zero to its maximum value  $I_{Lm}$  and at the same time the current through diode  $D$  is decreasing linearly. When the current of diode  $D$  becomes zero, the diode is reverse biased. Therefore, zero-current turn-on transition for  $S_r$  and zero-current turn-off transition for diode  $D$  are achieved. Using the equivalent circuit of Figure 2d, the following equations are obtained:

$$v_{cr}(t) = V_0 \quad (11)$$

$$i_{Lr}(t) = \frac{V_0}{L_r}(t - t_3) \quad (12)$$

$$v_{Lm}(t) = V_{in} - V_0 \quad (13)$$

This mode ends when  $i_{Lr}(t_4) = I_{Lm}$  and the time interval for this mode is given by:

$$t_{43} = t_4 - t_3 = \frac{I_{Lm}}{V_0} L_r \quad (14)$$

### MODE 5

$$t_4 < t < t_5 \quad (\text{Figure 2e})$$

This mode starts when diode  $D$  turns off at  $t = t_4$  and after this instance, a resonant circuit is formed consisting of the components  $L_r$ ,  $C_r$ ,  $S_r$  and  $D_r$ . Using the equivalent circuit of Figure 2e, the following equations are obtained:

$$v_{cr}(t) = V_0 \cos[\omega_r(t - t_4)] \quad (15)$$

$$i_{Lr}(t) = I_{Lm} + \frac{V_0}{Z_r} \sin[\omega_r(t - t_4)] \quad (16)$$

$$v_{Lm}(t) = V_{in} - V_0 \cos[\omega_r(t - t_4)] \quad (17)$$

Where

$$\omega_r = \frac{1}{\sqrt{L_r C_r}} = \text{Angular frequency of resonant tank} \quad (18)$$

$$Z_r = \sqrt{\frac{L_r}{C_r}} = \text{Impedance of the resonant tank} \quad (19)$$

This mode ends when  $i_{Lr}(t_5) = 0$  and therefore zero-current turn-off transition for  $S_r$  is achieved. The time interval of this mode is given by:

$$t_{54} = t_5 - t_4 = \frac{1}{\omega_r} \sin^{-1} \left( \frac{-I_{Lm} Z_r}{V_0} \right) \quad (20)$$

Finding a solution for equation (20) requires satisfaction of the following inequality.

$$I_{Lm} Z_r \leq V_0 \quad (21)$$

At the end of this mode  $v_{cr}(t_5) < 0$ .

### MODE 6

$$t_5 < t < t_6 \quad (\text{Figure 2f})$$

As soon as switch  $S_r$  and diode  $D_r$  stop conduction this mode begins. During this mode, the resonant capacitor  $C_r$  is charged linearly through the main inductor current  $I_{Lm}$ . The voltage across capacitor  $C_r$  is negative at the beginning of this mode and reaches zero at the instant  $t = t_6$  which is the end of this interval. Exactly at this instant switch  $S$  is turned on. Therefore, zero-voltage transition turn-on is achieved for the main switch. From the equivalent circuit of Figure 2f, the following equations are obtained:

$$v_{cr}(t) = V_0 \cos(\omega_r t_{54}) + \frac{I_{Lm}}{C_r}(t - t_5) \quad (22)$$

$$i_{Lr}(t) = 0 \quad (23)$$

$$v_{Lm}(t) = V_{in} - V_0 \cos(\omega_r t_{54}) - \frac{I_{Lm}}{C_r} (t - t_5) \quad (24)$$

This mode ends when  $v_{cr}(t_6) = 0$  and the time interval of this mode is given by:

$$t_{65} = t_6 - t_5 = \frac{V_{eq}}{I_{Lm}} C_r \quad (25)$$

Where

$$V_{eq} = \sqrt{V_0^2 - (I_{Lm} Z_r)^2} \quad (26)$$

Under steady-state conditions, the time integral of the main inductor voltage  $v_{Lm}$  over one switching cycle must be zero (Volt-second balance). Therefore,

$$\int_0^{T_s} v_{Lm}(t) dt = 0 \quad (27)$$

$$t_{32} = T_s - t_{10} - t_{21} - t_{43} - t_{54} - t_{65} \quad (28)$$

Using equations, (7), (14), (20), (25), (27), (28), (3), (6), (10), (13), (17) and (24) the required turn-on time of the main switch S can be calculated as:

$$t_{on1} = t_{10} = \frac{V_0 - V_{in}}{V_0} T_s - \frac{V_0}{2I_{Lm}} C_r - \frac{I_{Lm}}{V_0} L_r - \frac{1}{\omega_r} \sin^{-1} \left( \frac{-I_{Lm} Z_r}{V_0} \right) - \left( 2 + \frac{V_{eq}}{V_0} \right) \frac{V_{eq}}{2I_{Lm}} C_r \quad (29)$$

Using equations (7), (14), (20), (26) and (29) the time interval  $t_{32}$  can be calculated and is given by:

$$t_{32} = t_3 - t_2 = \frac{V_{in}}{V_0} T_s - \frac{V_0}{2I_{Lm}} C_r + \frac{V_{eq}^2}{2I_{Lm} V_0} C_r \quad (30)$$

Using equations (14) and (20) the required turn-on time of the auxiliary switch  $S_r$  can be calculated as:

$$t_{on2} = t_{43} + t_{54} = \frac{I_{Lm}}{V_0} L_r + \frac{1}{\omega_r} \sin^{-1} \left( \frac{-I_{Lm} Z_r}{V_0} \right) \quad (31)$$

The time delay  $t_d$  between the gating signals of the two switches (Figure 3) is calculated using equations (7) and (30) and is given by:

$$t_d = t_{21} + t_{32} = \frac{V_{in}}{V_0} T_s + \frac{V_0}{2I_{Lm}} C_r + \frac{V_{eq}^2}{2I_{Lm} V_0} C_r \quad (32)$$

The average current of the main inductor is given by

$$I_{Lm} = I_{in} \quad (33)$$

### III. THE GENERAL ACTIVE SNUBBER CELL FOR DC/DC CONVERTERS

The concept of the proposed active snubber cell for the boost converter can be extended to other DC/DC converters. The three remaining topologies (Buck, Buck-boost and Cuk) were analyzed with the waveforms of Figure 3. Figure 4 shows the four basic PWM converters with active snubber. The results of this analysis are reported in Table I.

### IV. DESIGN EXAMPLE

To verify the operation principles of the proposed active snubber cell, the following design specification for the boost converter is given here:

$$V_{in} = 9V, V_0 = 24V, I_0 = 0.1A \text{ and } f_s = 20kHz$$

The resonant frequency is chosen as  $f_r = 79.5kHz$

Using equation (33) and the above specifications, the main inductor current is found to be

$$I_{Lm} = 260mA$$

Taking into consideration equation (21), it is found that  $Z_r \leq 90\Omega$ . To ensure zero-current turn-off for the auxiliary switch,  $Z_r$  is chosen to be  $Z_r = 40\Omega$ .

Using equation (18) and (19), the following values for the elements of the resonant tank are found:

$$C_r = 50nF$$

$$L_r = 80\mu H$$

The time intervals for the six modes of operation are calculated using equations, (7), (14), (20), (25), (28) and (29):

$$t_{on1} = 15.5\mu sec$$

$$t_{21} = 4.5\mu sec$$

$$t_{32} = 18\mu sec$$

$$t_{43} = 0.8\mu sec$$

$$t_{54} = 7.2\mu sec$$

$$t_{65} = 4\mu sec$$

$$t_{on2} = 8\mu sec$$

$$t_d = 22.5\mu sec$$

### V. SIMULATED RESULTS

The results for this specific design example were obtained using the Pspice8 package and are presented in Figure 5. As can be seen, the simulated results are in close agreement with the theoretical ones.

### VI. EXPERIMENTAL RESULTS

The experimental waveforms of the designed converter are presented in Figure 6. It is clearly seen that the experimental results are in close agreement with the simulated ones.

### VII. CONCLUSION

In this paper, a general active snubber cell for DC/DC converters was proposed. To reduce switching losses and EMI noises, soft switching was applied to all semiconductor devices in the new converters.

The theoretical results for the proposed snubber were confirmed by both simulated and experimental results.

### REFERENCES

- [1]. N. Mohan, T. Undeland & W. Robbins, "Power Electronics: Converters, Applications and Design," John Wiley & sons, 1995.
- [2]. G. Hua, C. S. Leu, Y. Jiang, & F. C. Lee, "Novel Zero-Voltage Transition PWM Converters," *IEEE Trans. Power Electronics*, Vol. 9, No. 2, pp. 213-219, 1994.
- [3]. A. Elasser & D. A. Torrey, "Soft Switching Active Snubbers for DC/DC Converters," *IEEE Trans. Power Electronics*, Vol. 11, No. 5, pp. 710-722, 1996.
- [4]. Milan M. Jovanovic & Yungtaek Jang, "A Novel Active Snubber for High-Power Boost Converters," *IEEE Trans. Power Electronics*, Vol. 15, No. 2, pp 278-284, 2000.
- [5]. G. Hua, E. X. Yang, Y. Jiang, & F. C. Lee, "Novel Zero-Current Transition PWM Converters," *IEEE Trans. Power Electronics*, Vol. 9, No. 6, pp. 601-606, 1994.
- [6]. C. J. Tseng & C. L. Chen, "Novel ZVT-PWM Converters with Active Snubbers," *IEEE Trans. Power Electronics*, Vol. 13, No. 5, pp. 861-869, 1998.

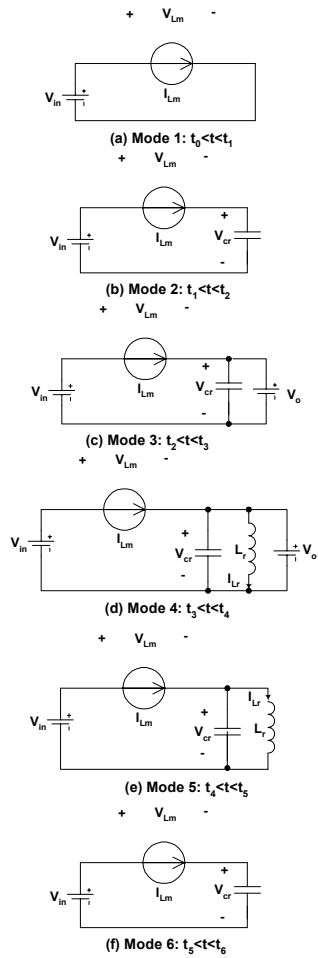


Fig.2. Equivalent circuits during one switching cycle

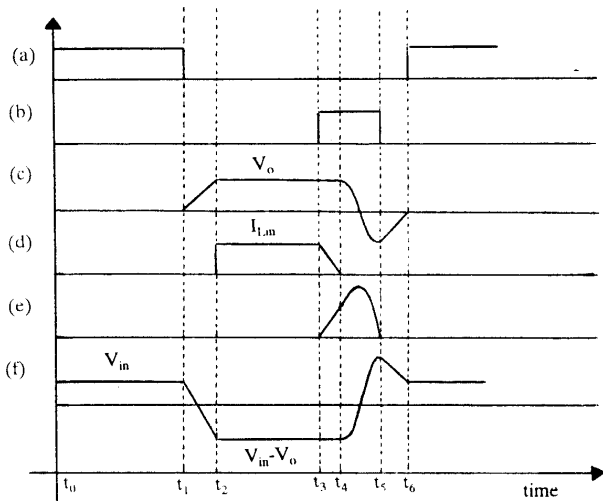


Figure 3. Key waveforms of the converter:  
 (a) Gating signal of  $S$ , (b) Gating signal of  $S_r$ ,  
 (c)  $v_{cr}(t)$ , (d)  $i_{Dr}(t)$ , (e)  $i_{Lr}(t)$  and (f)  $v_{Lm}(t)$ .

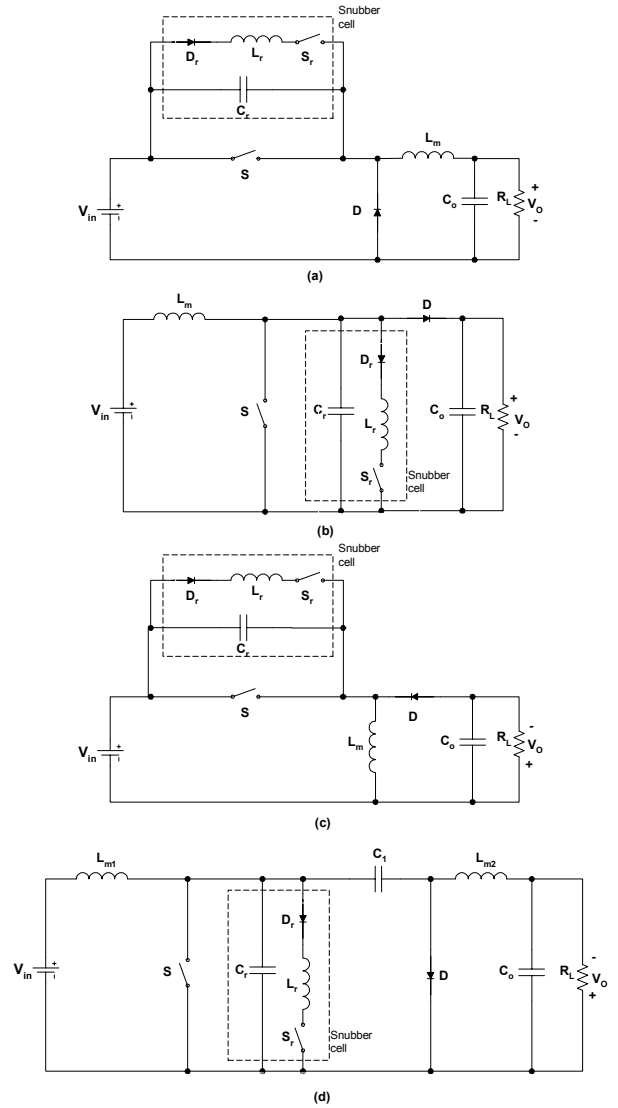


Fig.4. Four basic DC/DC converters with active snubber

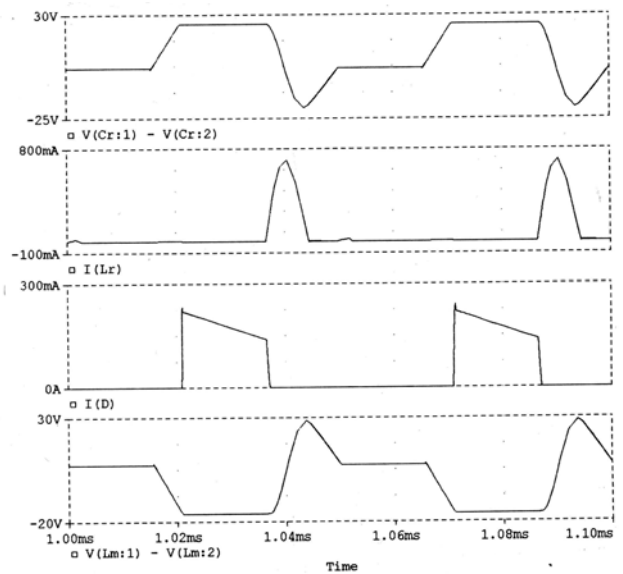


Fig.5. Simulated waveforms of the designed boost converter

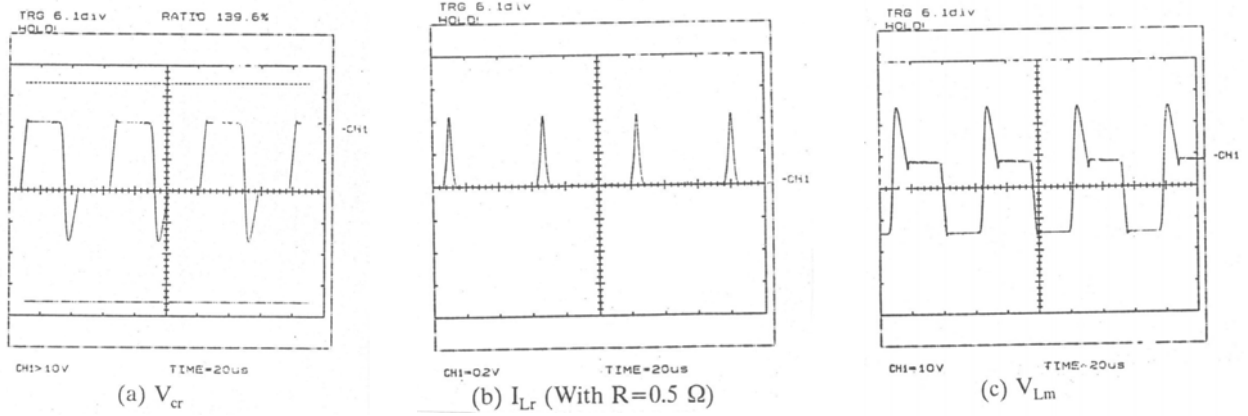


Fig.6. Experimental waveforms of the designed boost converter

Table I. Summary of the obtained results for the four basic DC/DC converters

	<b>Buck</b>	<b>Buck-boost</b>	<b>Cuk</b>
$t_{10}$	$\frac{V_0}{V_{in}} T_s - \frac{1}{2} t_{21} - t_{43}$ $-t_{54} - t_{65} - \frac{V_{eq}^2}{2I_{Lm} V_{in}} C_r$	$\frac{V_0}{V_{in} + V_0} T_s - \frac{1}{2} t_{21} - t_{43}$ $-t_{54} - t_{65} - \frac{V_{eq}^2}{2I_{Lm} (V_{in} + V_0)} C_r$	$\frac{V_0}{V_{in} + V_0} T_s - \frac{1}{2} t_{21} - t_{43}$ $-t_{54} - t_{65} - \frac{V_{eq}^2}{2I_{Lm} (V_{in} + V_0)} C_r$
$t_{21}$	$\frac{V_{in}}{I_{Lm}} C_r$	$\frac{V_{in} + V_0}{I_{Lm}} C_r$	$\frac{V_{in} + V_0}{I_{Lm}} C_r$
$t_{32}$	$\frac{V_{in} - V_0}{V_{in}} T_s - \frac{1}{2} t_{21}$ $+ \frac{V_{eq}^2}{2I_{Lm} V_{in}} C_r$	$\frac{V_{in}}{V_{in} + V_0} T_s - \frac{1}{2} t_{21}$ $+ \frac{V_{eq}^2}{2I_{Lm} (V_{in} + V_0)} C_r$	$\frac{V_{in}}{V_{in} + V_0} T_s - \frac{1}{2} t_{21}$ $+ \frac{V_{eq}^2}{2I_{Lm} (V_{in} + V_0)} C_r$
$t_{43}$	$\frac{I_{Lm}}{V_{in}} L_r$	$\frac{I_{Lm}}{V_{in} + V_0} L_r$	$\frac{I_{Lm}}{V_{in} + V_0} L_r$
$t_{54}$	$\frac{1}{\omega_r} \sin^{-1} \left[ \frac{-I_{Lm} Z_r}{V_{in}} \right]$	$\frac{1}{\omega_r} \sin^{-1} \left[ \frac{-I_{Lm} Z_r}{V_{in} + V_0} \right]$	$\frac{1}{\omega_r} \sin^{-1} \left[ \frac{-I_{Lm} Z_r}{V_{in} + V_0} \right]$
$t_{65}$	$\frac{V_{eq}}{I_{Lm}} C_r$	$\frac{V_{eq}}{I_{Lm}} C_r$	$\frac{V_{eq}}{I_{Lm}} C_r$
$V_{eq}$	$\sqrt{V_0^2 - (I_{Lm} Z_r)^2}$	$\sqrt{(V_{in} + V_0)^2 - (I_{Lm} Z_r)^2}$	$\sqrt{(V_{in} + V_0)^2 - (I_{Lm} Z_r)^2}$
$I_{Lm}$	$I_0$	$I_0 = I_{in}$	$I_0 = I_{in}$
$t_{on2}$	$t_{43} + t_{54}$	$t_{43} + t_{54}$	$t_{43} + t_{54}$
$t_d$	$t_{21} + t_{32}$	$t_{21} + t_{32}$	$t_{21} + t_{32}$